Bull. Mater. Sci., Vol. 31, No. 2, April 2008, pp. 121–124. © Indian Academy of Sciences.

Study of ferromagnetism in Mn-doped ZnO whisker arrays

FENG ZHU, YE ZHANG*, YOUGUO YAN, WENHAI SONG and LINGLI XIA†

Key Laboratory of Materials Physics, Institute of Solid State Physics, Hefei Institute of Physical Science, Chinese Academy of Sciences, Hefei 230031, P.R. China

†Basic Experiment Centre, Fundamental Department, Artillery Academy P.L.A

MS received 15 October 2007; revised 4 January 2008

Abstract. Vertically aligned Mn–ZnO whiskers were grown on sapphire substrate by a thermal chemical vapour deposition method. X-ray diffraction measurements indicate that samples are high-quality single crystals and *c*-axis oriented. Raman and XPS analyses revealed that Mn was incorporated into the ZnO lattice. Room temperature T_c ferromagnetism was observed. These Mn–ZnO whiskers may find their potential applications in spintronic field.

Keywords. ZnO; diluted magnetic semiconductors; chemical thermal deposition; spintronic; whisker.

1. Introduction

In recent years, diluted magnetic semiconductors (DMS) have attracted great attention due to their potential for the development of spintronic device (Kundaliya *et al* 2004; Kane *et al* 2005; Liu *et al* 2005; Luo *et al* 2005; Zhang *et al* 2005; Abouzaid *et al* 2006; Alaria *et al* 2006; Gu *et al* 2006; Hill *et al* 2006; Manivannan *et al* 2006; Ramachandran *et al* 2006; Wang *et al* 2006; Xu *et al* 2006). As to Dietl's theoretical prediction, p-type Mn-doped ZnO could keep ferromagnetism above room temperature (Dietl *et al* 2000). Many efforts have been made to investigate $Zn_{1-x}Mn_xO$ system. Also, Mn-doped ZnO with various morphologies, such as bulk (Kane *et al* 2005), films (Liu *et al* 2005; Abouzaid *et al* 2006; Gu *et al* 2006; Ramachandran *et al* 2006; Xu *et al* 2006) and nanoparticles (Luo *et al* 2005), have been prepared by different experimental methods. However, these magnetism results are inconsistent. For example, $Zn_{1-x}Mn_xO$ ($x = 0{\cdot}02$) synthesized by the sol–gel method are paramagnetic (Manivannan *et al* 2006). Meanwhile, Mn-doped zinc oxides synthesized by coprecipitation method display a typical paramagnetic behaviour (Alaria *et al* 2006). Bulk $Zn_{1-x}Mn_xO$ prepared by a melt-growth technique also shows a paramagnetic behaviour (Kane *et al* 2005). Whereas a few others have observed ferromagnetism of $Zn_{1-x}Mn_xO$ system (Jung *et al* 2002; Norton *et al* 2003; Sharma *et al* 2003; Heo *et al* 2004; Lim *et al* 2004; Ivill *et al* 2005; Kittilstved *et al* 2005). However, reports on ferromagnetism of one-dimensional $Zn_{1-x}Mn_xO$ system are very few. Recently, Jeong *et al* reported that they synthesized vertically well-aligned $Zn_{1-x}Mn_xO$ nanorod arrays with room temperature ferromagnetism by using a thermal chemical vapour deposition (CVD) process. In the preparation process, Au-coated sapphire was used as the substrate. In our paper, a CVD route was used to synthesize one-dimensional $Zn_{1-x}Mn_xO$ whisker arrays with room temperature ferromagnetism and the sapphire without Au coating was used as the substrate. The magnetic properties, structure and composition were investigated.

2. Experimental

In order to prepare Mn-doped ZnO whiskers, a mixture of Zn, ZnO, carbon and $MnCl_2$ powder (weight ratio of Zn, ZnO, carbon and $MnCl_2$ being 1 : 1 : 1 : 1) was loaded into an alumina boat to serve as the source material. Meanwhile, sapphire substrate was placed above the source at a vertical distance of about 5 mm with its polished side facing the source. The alumina boat was transferred into a horizontal alumina tube furnace, and then the furnace was heated up at a rate of 20°C/min under a constant Ar flow (flow rate: about 200 sccm; argon purity: 2% O_2 in Ar). The growth temperature was maintained at 950°C for 30 min, and then the furnace was allowed to cool down. A red thin layer of the as-prepared sample was found deposited on the entire sapphire. In design of source materials, the addition of ZnO and C will provide a continuous and stable oxygen supply through carbon-thermal reduction of ZnO. The high temperature reaction at 950°C is beneficial to Mn ions diffusing into Zn liquid droplets, which promote the formation of Mn-doping in Zn whiskers. The as-prepared samples were characterized by field emission scanning electron microscopy (SEM) (SEM: Sirion 200 FEG), X-ray diffraction spectra (XRD) (Philips

*Author for correspondence (yezhang@issp.ac.cn)

X'pert-PRO, CuKα (0·15419 nm) radiation) and X-ray photoelectronic spectroscopy (XPS). Raman scattering measurement was performed on a RAMANLOG 6 Raman system at backscattering geometry using the 514·53 nm line of an Ar^+ laser as excitation source. Magnetic measurements were performed using the quantum design physical property measurement system (PPMS).

3. Results and discussion

Figure 1 shows the XRD spectra of as-prepared sample. All diffraction peaks correspond to sapphire and wurtzite phases of ZnO. No trace of manganese related phase was detected. SEM image (figure 2) demonstrates that a large amount of whiskers were aligned onto sapphire substrate. Whiskers are hexagonal and well faceted. The surface of whisker is smooth and no nanoparticles are found to be attached to it. The diameter of whiskers range from 1–5 μm in length, about 10 μm.

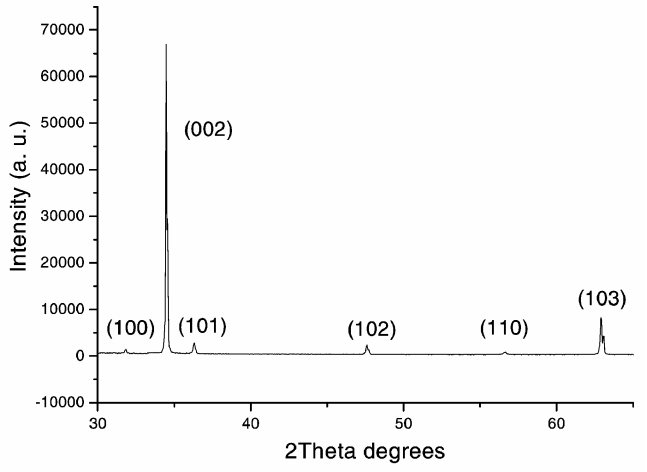

Figure 1. XRD spectra of Mn-doped ZnO whiskers.

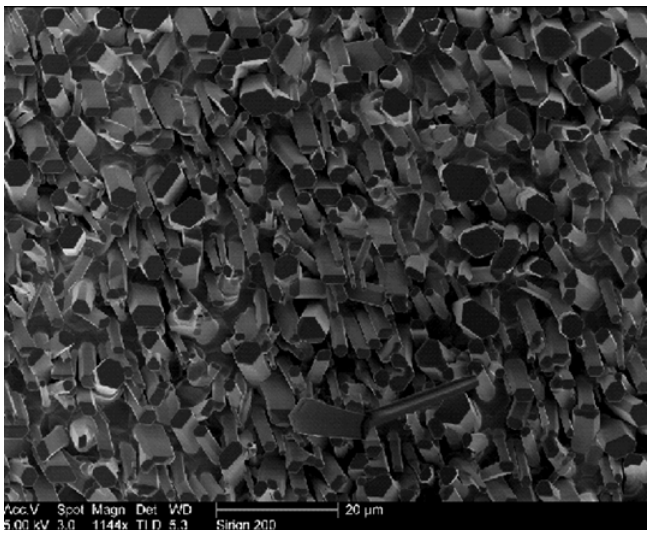

Figure 2. SEM image of Mn-doped ZnO whisker array.

X-ray photoelectronic spectroscopy (XPS) reveals that at. % of Zn, O and Mn of product are 40·62, 55·51 and 3·87, respectively. The percentage of Mn% is predecided by the vapour pressure of $MnCl_2$ at growth temperature. Figures 3a and b show the Zn and Mn 2*p* XPS spectra of as-prepared sample, respectively. They were calibrated by taking the carbon *C* 1*s* peak (binding energy = 284·6 eV) as reference. We can see from figure 3(a) that one strong peak appears at 1021·5 eV, which corresponds to the binding energies of Zn $2P_{3/2}$. The de-convoluted peak at 1022 eV corresponds to the binding energies of stoichiometric Zn ($2P_{3/2}$). The de-convoluted peak at 1021·25 eV corresponds to the binding energies of Zn with one broken bond. It is reasonable to consider that, due to the large size of Mn^{2+} compared to Zn^{+2} ion radius, Zn with broken bonds were introduced to the lattice. Figure 3(b) shows that one broad peak appears at 845·8 eV, which indicates the existence of Mn^{2+}.

The room temperature Raman spectra ranging from 200–1000 cm^{-1} are shown in figure 4. The strongest peak at about 435 cm^{-1} can be assigned to the high frequency branch of E_2 mode of ZnO, which is the strongest mode in wurtzite crystal structure. The full width at half maxi-

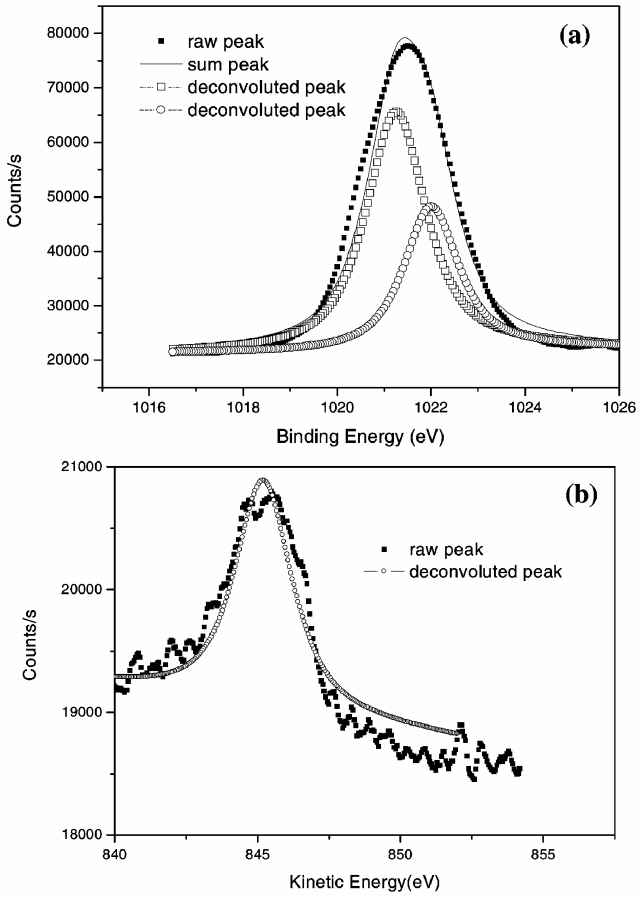

Figure 3. XPS spectra of Mn-doped ZnO whiskers: (**a**) Zn2p3scan and (**b**) Mn2p scan.

mum (FWHM) for this E_2 peak is 20 cm^{-1}, which implies that whiskers still keep good ZnO wurtzite structure under Mn doping. The peak at about 574 cm^{-1} can be assigned to A_1 longitudinal optical (LO) mode of ZnO. The peak at 326 cm^{-1} originates from the zone-boundary phonons of 2-$E_2(M)$ for ZnO. Another peak centred at 523 cm^{-1} has also been observed. Kaschner *et al* (2002), Cheng *et al* (2004) and Bundesmann *et al* (2003) also observed this mode in N, Ce- and Sb-doped ZnO. According to their explanation, this mode is induced by host lattice defects, such as oxygen vacancies and Zn interstitials. With the increment of doping content, the host lattice defects in ZnO are activated and amplified and then this mode (523 cm^{-1}) appears. In our case, this is attributed to the larger size of Mn^{2+} (1·10 Å) compared to Zn^{2+} ionic radius (0·89 Å). When Mn^{2+} was doped into ZnO lattice, new lattice defects, such as oxygen vacancies and Zn interstitials, are created. Therefore, the appearance of 523 cm^{-1} can be used to characterize Mn^{2+} doped into ZnO lattice. Compared with those of bulk ZnO, all Raman shifts exhibit red shifts. The red shifts indicate that whiskers are under a tensile force.

Figure 5(a, b) shows the field-dependent magnetization curves (M–H curve) of Mn-doped ZnO whiskers at 7 K and room temperature, respectively. Hysteresis loop behaviour is observed at 7 K and room temperatures with the coercive field of 114 Oe and 58 Oe, respectively. The magnetization at room temperature is relatively weak. The magnetic signal from the sapphire substrate was subtracted in these measurements. However, for ZnO whiskers without doping, no hysteresis loop behaviour appears. These results confirm that Mn doping into ZnO lattice can induce ferromagnetic ordering at room temperature. Temperature-dependent magnetization, M vs T measurements of Mn-doped ZnO whiskers were performed under both zero-field-cooled (ZFC) and field-cooled (FC) conditions. As shown in figure 5c, a deviation of ZFC and FC magnetizations exist up to 300 K. This magnetization difference can be attributed to the following: For FC sample at room temperature, the ferromagnetic ordering appears obviously under the magnetic field of 1T. When the temperature decreases from 300 to 7 K, the ferromagnetic ordering degree becomes low. Until 7K, the ferromagnetic ordering degree still keeps a higher value, but for ZFC sample, from room temperature to 7 K, the sam-

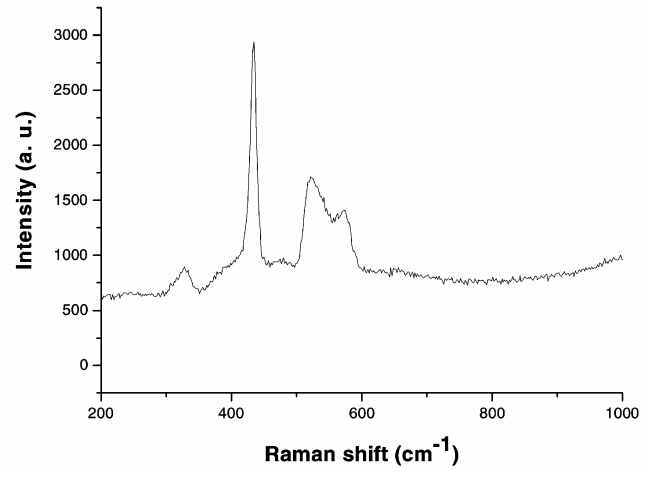

Figure 4. Raman spectra of Mn-doped ZnO whiskers.

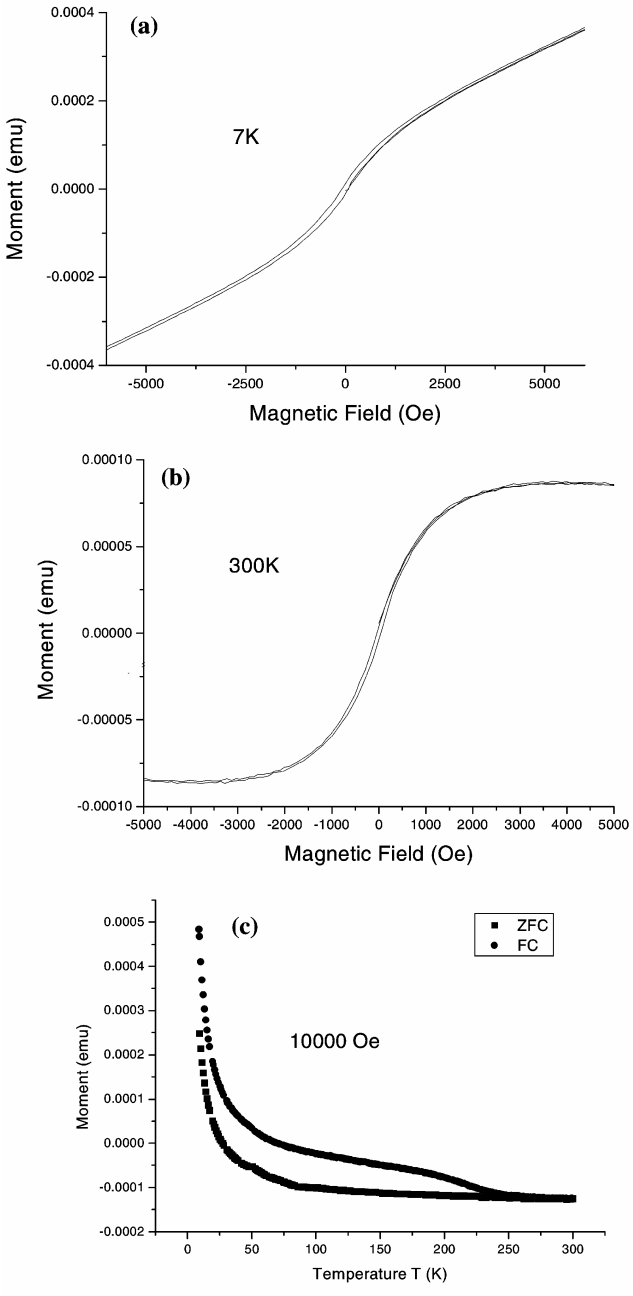

Figure 5. (**a**) M–H relationship of Mn-doped ZnO whiskers at 7 K, (**b**) M–H relationship of Mn-doped ZnO whiskers at 300 K and (**c**) temperature dependent magnification (M–T) curves of Mn-doped ZnO whiskers at a magnetic field of 10000 Oe (ZFC and ZF).

ple has not been magnetized. When the temperature reaches 7 K, the ferromagnetic ordering takes place under magnetic field of 1*T*. Because the temperature is very low, this is not beneficial to ferromagnetic ordering, and thus the ferromagnetic ordering is carried out slowly. As a result the ferromagnetic ordering degree is lower than that of FC sample, as shown in figure 5c. When the temperature rises, for FC and ZFC samples the thermal action makes the ferromagnetic ordering degree to decrease. Therefore, the magnetization difference between FC and ZFC samples is kept from 7 K to 300 K.

4. Conclusions

In conclusion, Mn-doped ZnO whisker arrays were fabricated on sapphire substrate via a thermal chemical vapour deposition method. Mn-doped whiskers array were *c*-axis oriented and well-aligned. Mn-doping introduces the lattice defects and induces Raman vibration modes at 523 cm^{-1}. Room temperature T_c ferromagnetism is observed. Mn-doped whiskers may have potential future in spintronic applications.

Acknowledgements

We acknowledge the support from the National Key Project of Fundamental Research for Nanomaterials and Nanostructures (Grant No. 2005CB623603) and the Natural Science Foundation of Anhui (Grant No. 070414196).

References

Abouzaid M, Ruterana P, Liu C and Morkoc H 2006 *J. Appl. Phys.* **99** 113515

Alaria J, Bouloudenine M, Schmerber G, Colis S, Dinia A, Turek P and Bernard M 2006 *J. Appl. Phys.* **99** 08M118

Bundesmann C, Ashkenov N, Schubert M, Spemann D, Butz T, Kaidashev E M, Lorenz M and Grundmann M 2003 *Appl. Phys. Lett.* **83** 1974

Cheng B C, Xiao Y H, Wu G S and Zhang L D 2004 *Appl. Phys. Lett.* **84** 416

Dietl T, Ohno H, Matsukura F, Cibert J and Ferrand D 2000 *Science* **287** 1019

Gu Z B *et al* 2006 *Appl. Phys. Lett.* **88** 082111

Heo Y W *et al* 2004 *Appl. Phys. Lett.* **84** 2292

Hill D H *et al* 2006 *Phys. Status Solidi* **203** 3836

Ivill M, Pearton S J, Norton D P, Kelly J and Hebard A F 2005 *J. Appl. Phys.* **97** 053904

Jung S W, An S J, Yi G, Jung C U, Lee S and Cho S 2002 *Appl. Phys. Lett.* **80** 4561

Kane M H, Shalini K, Summers C J, Varatharajan R, Nause J, Vestal C R, Zhang Z J and Ferguson I T 2005 *J. Appl. Phys.* **97** 023906

Kaschner A *et al* 2002 *Appl. Phys. Lett.* **80** 1909

Kittilstved K R, Norberg N S and Gamelin D R 2005 *Phys. Rev. Lett.* **94** 147209

Kundaliya D C *et al* 2004 *Nature* **3** 709

Lim S W, Jeong M C, Ham M H and Myoung J M 2004 *Jpn J. Appl. Phys.* **43** L280

Liu C *et al* 2005 *J. Appl. Phys.* **97** 126107

Luo J, Liang J K, Liu Q L, Liu F S, Zhang Y, Sun B J and Rao G H 2005 *J. Appl. Phys.* **97** 086106

Manivannan A, Dutta P, Glaspell G and Seehra M S 2006 *J. Appl. Phys.* **99** 08M110

Norton D P, Pearton S J, Hebard A F, Theodoropoulou N, Boatner I A and Wilson R G 2003 *Appl. Phys. Lett.* **82** 239

Ramachandran S, Narayan J and Prater J T 2006 *Appl. Phys. Lett.* **88** 242503

Sharma P *et al* 2003 *Nat. Mater.* **2** 673

Wang J B, Huang G J, Zhong X L, Sun L Z, Zhou Y C and Liu E H 2006 *Appl. Phys. Lett.* **88** 252502

Xu H Y, Liu Y C, Xu C S, Liu Y X, Shao C L and Mu R 2006 *Appl. Phys. Lett.* **88** 242502

Yadav H K, Sreenivas K and Gupta V J 2006 *Appl. Phys.* **99** 083507

Zhang J, Skomski R J and Sellmyer D 2005 *J. Appl. Phys.* **97** 10D303